INSTITUTO DE FÍSICA

preprint

IFUSP/P-220

FORWARD OPTICAL GLORY

by

H.M. Nussenzveig

Instituto de Física, Universidade de São Paulo,
São Paulo, Brazil

and

W.J. Wiscombe

National Center for Atmospheric Research,
Boulder, Colo. 80307

UNIVERSIDADE DE SÃO PAULO
INSTITUTO DE FÍSICA
Caixa Postal - 20.516
Cidade Universitária
São Paulo - BRASIL

Forward Optical Glory

H.M. Nussenzveig

Instituto de Física, Universidade de São Paulo, Brazil

and

W.J. Wiscombe

National Center for Atmospheric Research*, Boulder, Colo. 80307

ABSTRACT

Forward optical glory effects in Mie scattering are displayed here for the first time. These effects include regular oscillations in Mie efficiency factors and characteristic deviations from zero polarization in near-forward scattering which are observable for real refractive indices near $\sqrt{2}$ and 2. Complex angular momentum theory predicts the period of oscillation correctly and shows the important role played by surface waves with shortcuts through the sphere. Three possible types of experiments for detecting the forward glory are proposed, involving measurements of extinction, radiation pressure, and polarization in near-forward scattering.

---

* The National Center for Atmospheric Research is sponsored by the National Science Foundation.

The usual optical glory consists of a strong enhancement in near-backward scattering of visible light from water droplets with size parameter $\beta = ka \gtrsim 10^2$ (k = wave number; a = droplet radius). It results[1,2] from a complicated interplay of several effects produced by near-grazing incident rays, including interference between diffracted rays associated with surface waves and complex rays in the shadow of high-order rainbows.

In any type of spherically symmetric scattering, a "glory ray" is defined as a non-axial trajectory that emerges in the exactly forward or backward direction. Glory scattering in this sense produces an intensity enhancement, due to the axial focusing effect[3]. For the refractive index of water, no real glory rays of significant intensity (i.e., associated with a small number of internal reflections) exist[3]: the effect is due to complex trajectories.

Interference between forward glory rays and the forward diffraction peak leads to an oscillatory behavior of the total cross section as a function of β. This phenomenon, known as "glory undulations" or "glorified shadow", was predicted[4] and observed[5] in atom-atom scattering. In order to obtain an observable forward glory in Mie scattering, several conditions must be met:

(i) the contributing paths should involve the fewest possible number of internal reflections in order to minimize the damping by internal reflections and by absorption along the optical path inside the sphere (associated with the imaginary part κ of the complex refractive index $N = n + i\kappa$);

(ii) the paths should arise from near-tangential incident rays[2]

in order to lose the least amount of energy at each internal reflection;

(iii) the effect must be large enough to be seen over the intense forward diffraction peak, which normally swamps the other contributions to near-forward scattering.

The smallest number of internal reflections that can lead to a real forward glory ray is two, requiring a real refractive index $n \geq 2$. For $n = 2$, this corresponds to tangential incidence and to an equilateral triangle inscribed within the sphere. It is the lowest "geometrical resonance"[6]. For a material with $n < 2$, the triangle does not quite close, as shown in Fig. 1: there remains an angular gap ζ to be bridged by surface waves, given by

$$\zeta = 6 \sin^{-1}(1/n) - \pi \quad , \tag{1}$$

and amounting to approximately 16^{o} for $n = 1.85$, 10.5^{o} for $n = 1.90$ and 5^{o} for $n = 1.95$.

That this gap is indeed being bridged can be seen from Fig. 2, which shows the exact Mie extinction efficiency $Q_{ext}(N,\beta)$ for $N = 1.9 + 10^{-4}\, i$ and $500 \leq \beta \leq 505$, compared to the asymptotic approximation $Q_{ext}^{as}(N,\beta)$ derived from complex angular momentum theory[7], up to $O(\beta^{-2})$, excluding "ripple" contributions. The difference $Q_{ext} - Q_{ext}^{as}$ does not show the usual irregular ripple fluctuations (apart from some minor residual components), but rather a regular, nearly sinusoidal oscillation. This represents glory undulations, arising from interference between the forward diffraction peak and forward glory contributions of the type illustrated in Fig. 1.

The effect appears even more strikingly in Fig. 3, which shows the exact Mie radiation pressure efficiency $Q_{pr}(N,\beta)$ in the same range

along with the asymptotic approximation [7] to its average value $< Q_{pr}^{as}(N,\beta) >$ over an interval $\Delta\beta = \pi$.

In these examples the forward glory effect appears in an especially pure form: interference with other terms in the Debye multiple internal reflection expansion[2] is damped out by the imaginary index κ. We have plotted many other such examples for the ranges $1.8 \leq n \leq 2.05$, $10^{-7} \leq \kappa \leq 10^{-2}$, and $50 \lesssim \beta \lesssim 1500$. The forward glory oscillations appear very clearly in all Mie efficiency factors, including those for scattering and absorption. For smaller values of $\kappa\beta$, the amplitude of the glory oscillations increases, but at the same time the admixture with other ripple components becomes more evident, particularly for the absorption efficiency.

From these graphs, the period $(\delta\beta)_{Mie}$ of the forward glory oscillations can be estimated with an accuracy of the order of 0.001. The theoretical expression for the period derived from complex angular momentum (CAM) theory is

$$(\delta\beta)_{CAM} = 2\pi/(6\sqrt{n^2-1} + \zeta) \quad . \tag{2}$$

Table I shows a comparison between the theoretical period and that measured from the graphs. The agreement is excellent.

There are several possibilities for the experimental detection of the forward glory effect. A variety of very dense liquids and glasses have refractive indices in the range $1.8 \lesssim n \lesssim 2.0$ with not too large κ, so that either liquid droplets or solid spheres may be employed. Possible experiments include:

(a) Extinction: Accurate extinction measurements are difficult. The most favorable range to detect the glory oscillations would be

$50 \lesssim \beta \lesssim 150$, where their amplitude reaches several percent of Q_{ext} if $\kappa \lesssim 10^{-4}$, dropping to <1% if $\kappa \gtrsim 10^{-3}$. In the case shown in Fig. 2, the relative amplitude is ~0.3%.

(b) Radiation pressure: Within the same range as in (a), the relative amplitude of the glory oscillations in the radiation pressure efficiency reaches up to ~20%, so that they should be readily detectable. The radiation pressure may be accurately measured by Ashkin and Dziedzic's beautiful levitation technique[8].

(c) Polarization in near-forward scattering: For scattering angles $\theta << \beta^{-1/3}$ and $u = \beta\theta$ not >> 1, both scattering amplitudes tend to be dominated by the well-known Airy pattern of Fraunhofer diffraction by a circular disc, $J_1(u)/u$ (J_1 = Bessel function of order one), which gives rise to the forward diffraction peak. The forward glory polarized amplitudes, analogously to the backward glory ones[2], contain one component with the same Airy pattern behavior and another one with angular dependence given by $J_1'(u)$. Interference with the glory amplitudes produces small corrections to the Airy pattern, mainly in the form of a slight intensity oscillation within the central Airy bright ring.

Polarization effects should be more readily detected. The forward glory contribution is strongly polarized, with dominance of the electric (parallel) component, as is characteristic for surface waves[2]. However, because of the relatively small amplitude ($\lesssim \beta^{-2/3}$) of the glory contribution with respect to the (unpolarized) forward diffraction peak, one must look for an interference effect between these two contributions.

The interference term in $i_1 - i_2$ (i_1 = perpendicular polarized intensity; i_2 = parallel polarized intensity) is proportional to

$J_2(u)\ J_1(u)/u$, whereas $i_1 + i_2$ is dominated by the Airy term $[J_1(u)/u]^2$ except near zeros of $J_1(u)$, where $\mathcal{O}(\beta^{-2/3})$ terms contribute. It follows that the degree of polarization $P = (i_1-i_2)/(i_1+i_2)$ starts out from zero at $\theta = 0$ and goes through a peak (positive or negative, following the glory oscillations[9]) just before vanishing near $u = 3.83$ [first zero of $J_1(u)$]; it then changes sign in most cases, going through another peak of opposite sign shortly thereafter and then decreasing to go through the next zero near $u = 5.14$ [first zero of $J_2(u)$].

The forward glory may therefore be detected by observing the two polarization peaks of opposite signs in the range of $3 \lesssim \beta\theta \lesssim 4.5$ and their characteristic oscillatory dependence[9]. (Note that the total intensity $(i_1 + i_2)$ is rather low near the peaks because this is the region where the first minimum in the Airy diffraction pattern occurs). An example of this behavior is shown in Fig. 4. It should be remarked, however, that not all cases are as clear-cut as Fig. 4. Not infrequently one of the peaks will be very much smaller than the other one, or the pattern for $\beta + 1/2(\delta\beta)_{CAM}$ will not look much like the sign-flipped version of the pattern for β. Therefore, if this test is to be useful experimentally, a large sample of β's will be required, and one will have to look at the preponderance of evidence rather than isolated examples.

The following remarks apply to all three proposed experimental tests:

(i) The size parameter fluctuation $\Delta\beta$ in the experiment must be $<< \delta\beta$, the period of the glory oscillations, in order not to wash out the interference.

(ii) The imaginary index κ must be such that $\kappa\beta \ll 1$ to avoid strong absorption damping.

(iii) The value of β should be as small as feasible within the range $50 \lesssim \beta \lesssim 10^3$ to reduce surface wave damping of the glory amplitude.

(iv) One may vary either the wavelength λ or the radius a (by evaporation of a droplet) to change β, but in the former case dispersion should be weak enough to avoid significant change in n.

The near-backward angular distribution in the proposed experiments is also of interest. Indeed, as $n \to 2$, the rainbow angle θ_R of the primary bow approaches [6] 180°, so that the rainbow enhancement (of order $\beta^{1/6}$) combines with the axial focusing enhancement (of order $\beta^{1/2}$) to give an overall backward enhancement [2] of order $\beta^{2/3}$; this leads to strong backward peaking [10] of the intensity.

The next geometrical resonance (inscribed square [6]) occurs at $n = \sqrt{2}$. The corresponding forward glory, with period

$$(\delta\beta)'_{CAM} = 2\pi/(8\sqrt{n^2-1} + \zeta'),$$

$$\zeta' \equiv 8 \sin^{-1}(1/n) - 2\pi ,$$

should have appreciably lower amplitude (primarily because of the extra damping associated with an extra internal reflection). However, one may look for it in the range $1.4 \leq n \leq 1.45$, which is more readily accessible. We have verified that the exact degree of polarization P for n = 1.4 shows a pattern like that of Fig. 4 and that the various efficiency factors exhibit smooth oscillations whose period is in excellent agreement with $(\delta\beta)'_{CAM} \simeq 0.8$.

Footnotes and References

1. V. Khare and H.M. Nussenzveig, "Theory of the Glory", Phys. Rev. Lett. 38, 1279-1282 (1977).
2. H.M. Nussenzveig, "Complex Angular Momentum Theory of the Rainbow and the Glory", J. Opt. Soc. Am. 69, 1068-1079 (1979).
3. H.C. van de Hulst, Light Scattering by Small Particles (Wiley, New York, 1957), p. 250.
4. R.B. Bernstein, "Calculation of the Velocity Dependence of the Differential and Total Cross Sections for Elastic Scattering of Molecular Beams", J. Chem. Phys. 34, 361-365 (1961).
5. E.W. Rothe, P.K. Rol, S.M. Trujillo and R.H. Neynaber, "Velocity Dependence of the Total Cross Section for the Scattering of Li and K by Xe", Phys. Rev. 128, 659-662 (1962).
6. H.M. Nussenzveig, "High-Frequency Scattering by a Transparent Sphere. II. Theory of the Rainbow and the Glory", J. Math. Phys. 10, 125-176 (1969).
7. H.M. Nussenzveig and W.J. Wiscombe, "Efficiency Factors in Mie Scattering", submitted for publication.
8. A. Ashkin and J.M. Dziedzic, "Observation of Resonances in the Radiation Pressure on Dielectric Spheres", Phys. Rev. Lett. 38, 1351-1354 (1977).
9. The pattern of P tends to flip sign when β increases by half a glory oscillation period ($\beta \to \beta + 1/2\ \delta\beta$).
10. P. Pechukas, "Time-Dependent Semiclassical Scattering Theory", Phys. Rev. 181, 166-174 (1969).

Table I. Comparison between Glory Oscillation Periods

Predicted by Mie Theory and by Complex Angular Momentum Theory

n	1.85	1.90	1.95	2.00
$(\delta\beta)_{CAM}$	0.6529	0.6361	0.6200	0.6046
$(\delta\beta)_{Mie}$	0.653	0.636	0.620	0.604

Figure Captions

Fig. 1 Contribution to the forward glory due to a tangentially incident ray IT. The path C T G corresponds to a diffracted ray that travels along CT as a surface wave. Portions of surface wave paths can also be described around T, A and B, but the arcs travelled must add up to $\zeta = 6\theta_\ell - \pi$, where $\theta_\ell = \sin^{-1}(1/n)$ is the critical angle.

Fig. 2 Exact (Q_{ext}) and asymptotic (Q^{as}_{ext}) Mie extinction efficiencies for refractive index $N = 1.9 + 10^{-4}i$ and size parameter range $500 \leq \beta \leq 505$.

Fig. 3 Exact (Q_{pr}) and asymptotic ($\langle Q^{as}_{pr} \rangle$, averaged over $\Delta\beta = \pi$) Mie radiation pressure efficiencies for refractive index $N = 1.9 + 10^{-4}i$ and size parameter range $500 \leq \beta \leq 505$.

Fig. 4 Exact Mie percent polarization 100P vs. $\beta\theta$ for refractive index $N = 1.9 + 10^{-6}i$ and size parameters $\beta = 300$ and $\beta + 1/2(\delta\beta)_{CAM} = 300.318$ (θ = scattering angle in radians).

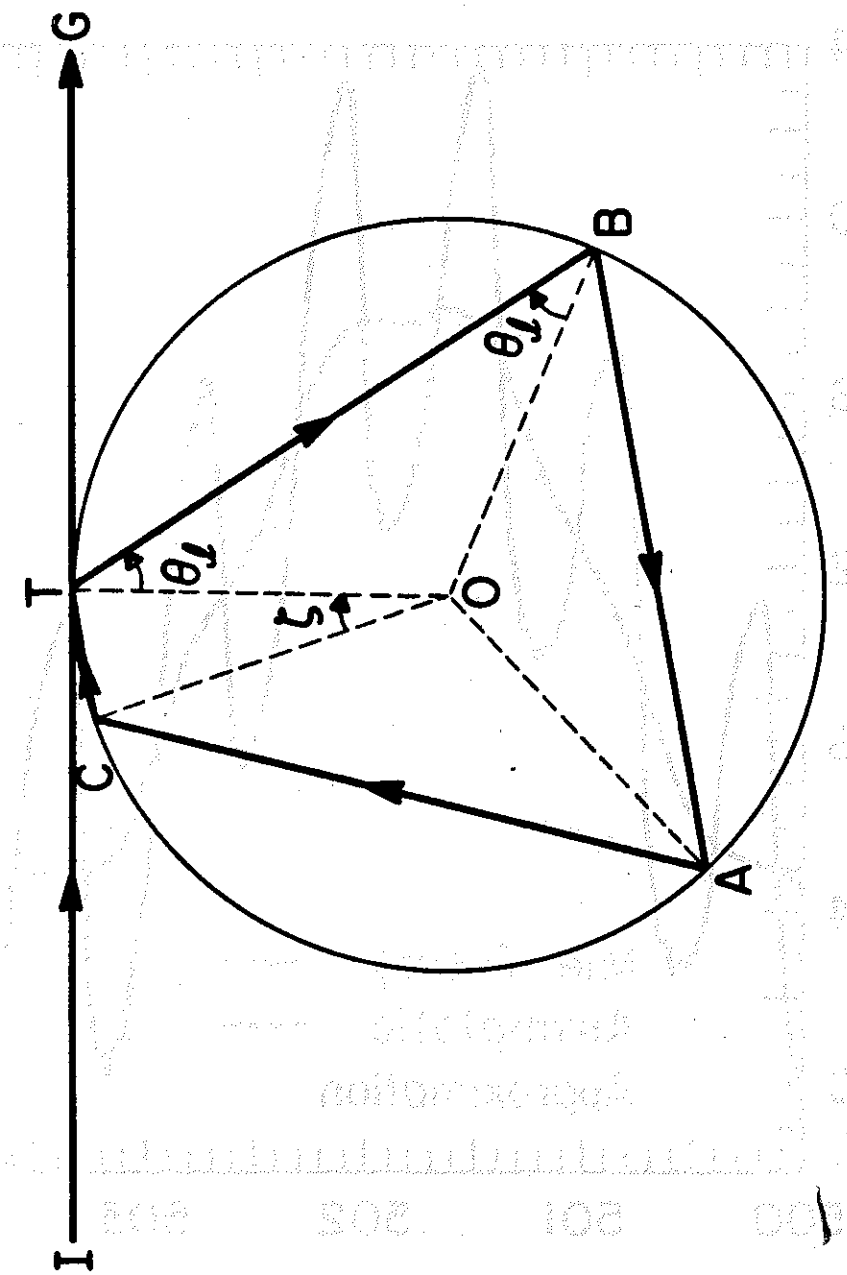

Fig. 1

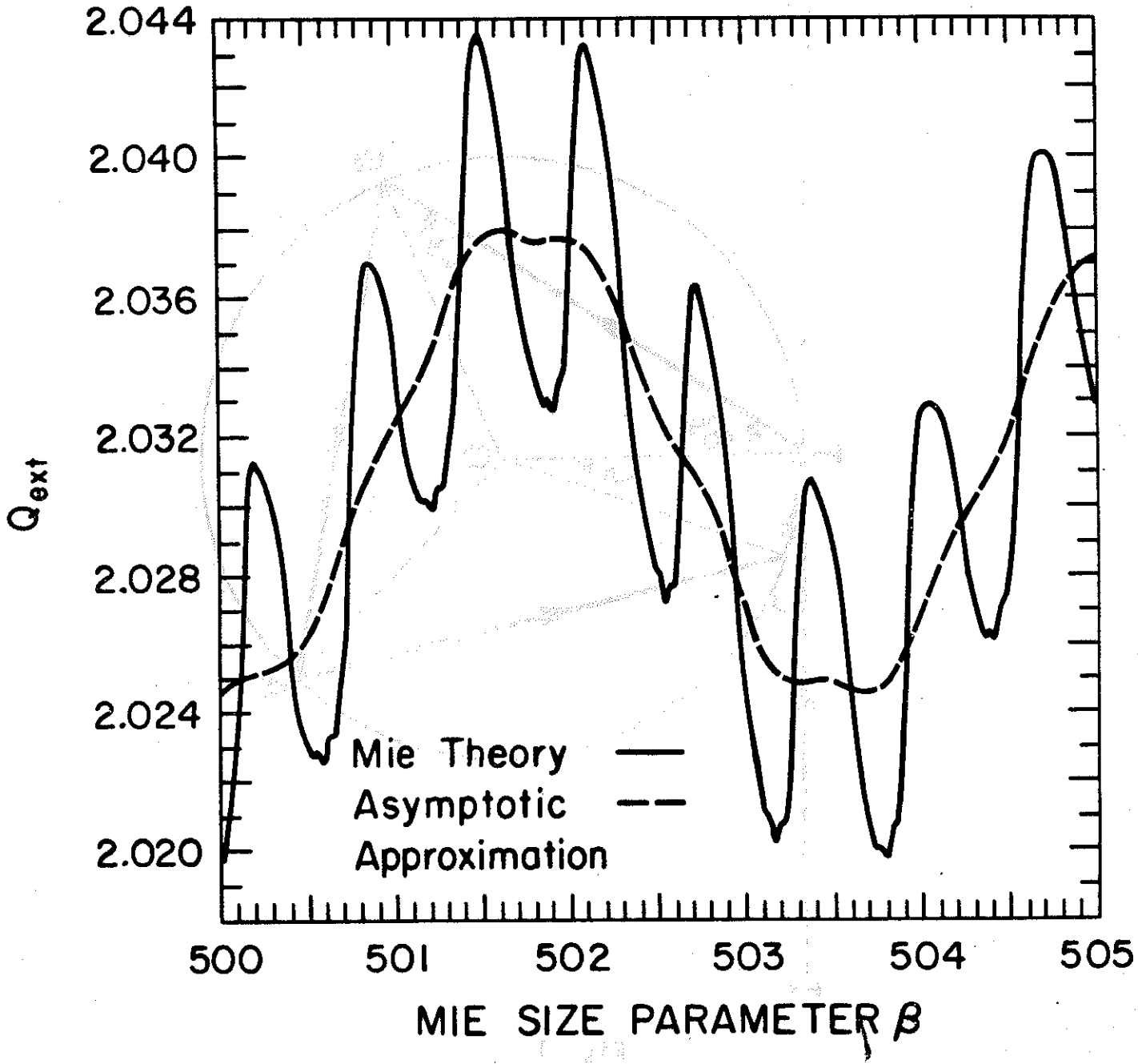
2.044
2.040
2.036
2.032
2.028
2.024
2.020
Q_{ext}
Mie Theory
Asymptotic
Approximation
500
501
502
503
504
505
MIE SIZE PARAMETER β

Fig. 2

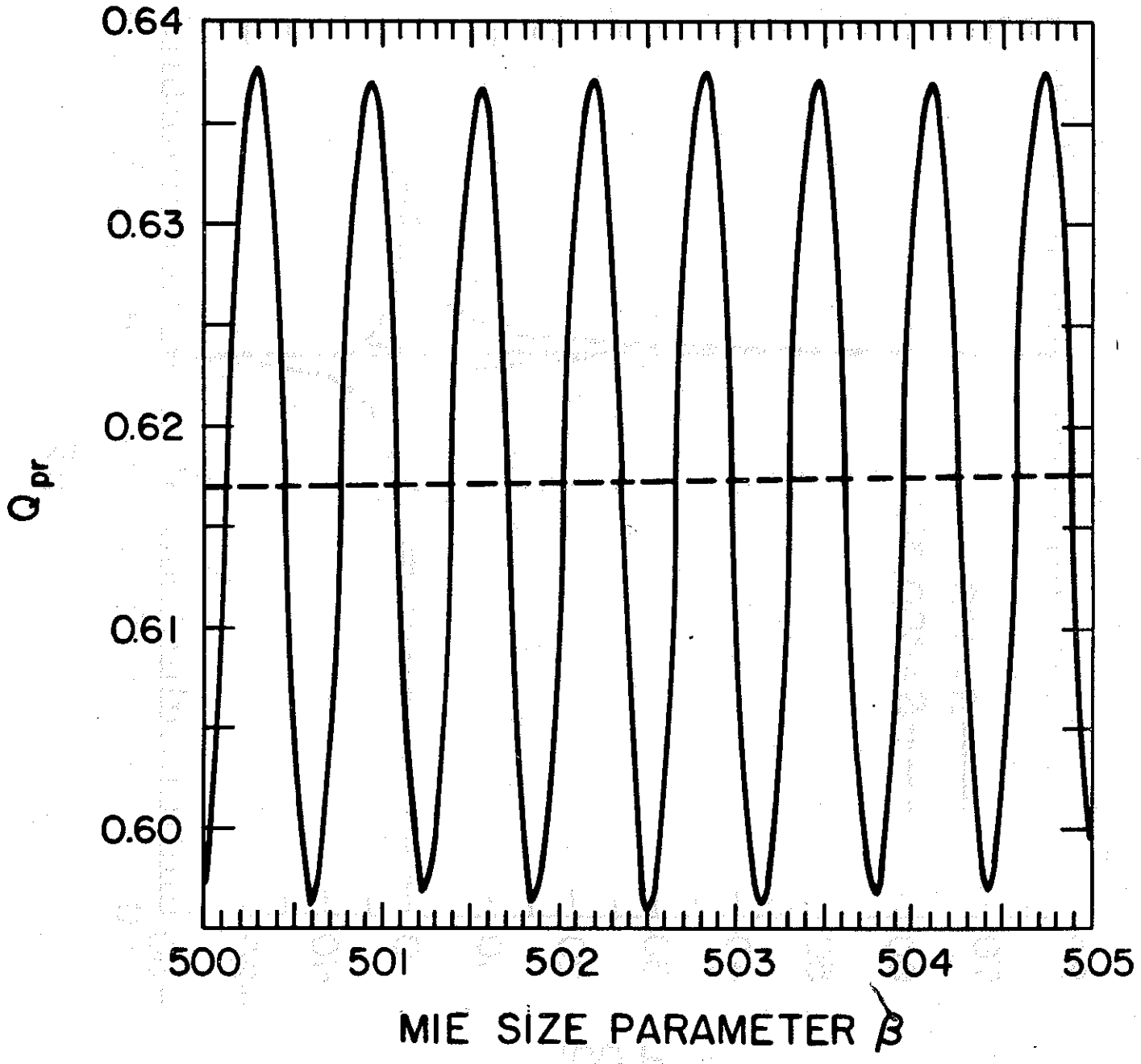
0.64
0.63
0.62
0.61
0.60
Q_{pr}
500
501
502
503
504
505
MIE SIZE PARAMETER β

Fig. 3

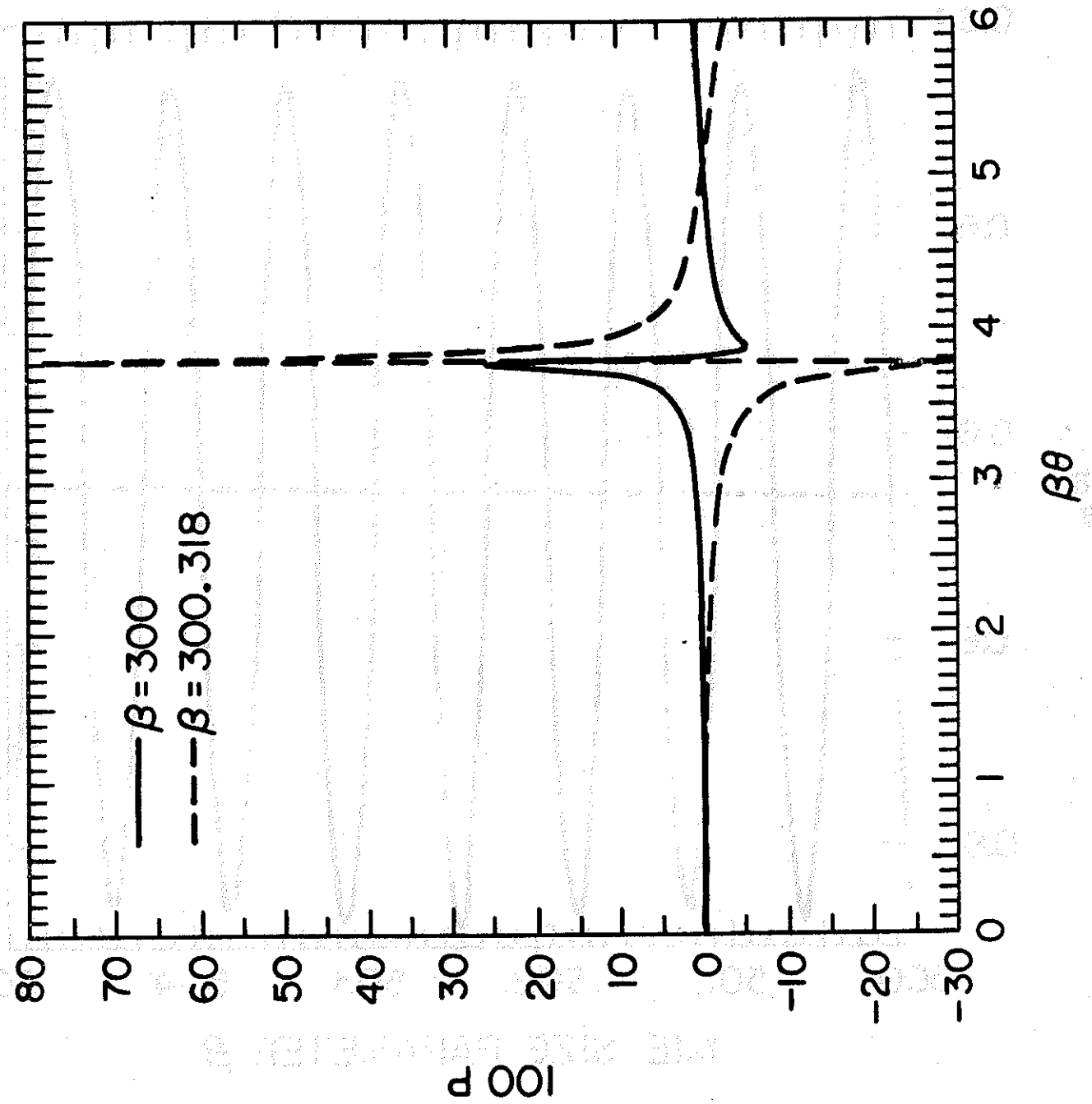

Fig. 4